Catalysts **2014**, *4*, 276-288; doi:10.3390/catal4030276

OPEN ACCESS

catalysts

ISSN 2073-4344

www.mdpi.com/journal/catalysts

Article

Selective Hydrogenation of *m*-Dinitrobenzene to *m*-Nitroaniline over Ru-SnO_x/Al_2O_3 Catalyst

Haiyang Cheng [1,2], Weiwei Lin [2], Xiaoru Li [2], Chao Zhang [2] and Fengyu Zhao [1,2,*]

[1] State Key Laboratory of Electroanalytical Chemistry, Changchun Institute of Applied Chemistry, Chinese Academy of Sciences, Changchun 130022, China

[2] Laboratory of Green Chemistry and Process, Changchun Institute of Applied Chemistry, Chinese Academy of Sciences, Changchun 130022, China; E-Mails: hycyl@ciac.ac.cn (H.C.); linwei@ciac.ac.cn (W.L.); lixiaoru@ciac.ac.cn (X.L.); czhang@ciac.ac.cn (C.Z.)

* Author to whom correspondence should be addressed; E-Mail: zhaofy@ciac.ac.cn; Tel./Fax: +86-431-8526-2410.

Received: 19 May 2014; in revised form: 23 June 2014 / Accepted: 25 June 2014 / Published: 14 July 2014

Abstract: Series catalysts of Ru-SnO_x/Al_2O_3 with varying SnO_x loading of 0–3 wt% were prepared, and their catalytic activity and selectivity have been discussed and compared for the selective hydrogenation of *m*-dinitrobenzene (*m*-DNB) to *m*-nitroaniline (*m*-NAN). The Ru-SnO_x/Al_2O_3 catalysts were characterized by X-ray powder diffraction (XRD), X-ray photoelectron spectroscopy (XPS), transmission electron microscopy (TEM) and hydrogen temperature-programmed reduction (H_2-TPR) and desorption (H_2-TPD). Under the modification of SnO_x, the reaction activity increased obviously, and the best selectivity to *m*-NAN reached above 97% at the complete conversion of *m*-DNB. With the increasing of the SnO_x loading, the amount of active hydrogen adsorption on the surface of the catalyst increased according to the H_2-TPD analysis, and the electron transferred from Ru to SnO_x species, as determined by XPS, inducing an electron-deficient Ru, which is a benefit for the absorption of the nitro group. Therefore, the reaction rate and product selectivity were greatly enhanced. Moreover, the Ru-SnO_x/Al_2O_3 catalyst presented high stability: it could be recycled four times without any loss in activity and selectivity.

Keywords: Ru catalyst; SnO_x doping; hydrogenation; *m*-dinitrobenzene; *m*-nitroaniline; catalyst recycling

1. Introduction

m-Nitroaniline (*m*-NAN) is an important intermediate for the preparation of dyes, mechanical and electronic corrosion inhibitors, urethanes and pharmaceuticals. Generally, *m*-NAN is produced from the partial reduction of *m*-dinitrobenzene (*m*-DNB) with disulfides or metal acid systems and produced by the acetylation of aniline and then nitration, with subsequent removal of the acetyl group by hydrolysis. Both of these two methods are hazardous, tedious and costly, with further separation and waste disposal. From environmental and economic points of view, catalytic, selective hydrogenation of *m*-DNB directly to *m*-NAN should be an attractive process, and it has attracted much attention in recent years [1–3]. However, controlling the product selectivity is particularly a challenge in the hydrogenation of *m*-DNB in terms of the exclusive formation of *m*-NAN (partial reduction product), due to it being easily hydrogenated to the complete reduction product of *m*-phenylenediamine (*m*-PDA) [4,5] and the formation and accumulation of intermediates, such as phenylhydroxylamine (PHA), azoxy-benzene (AOB), azo-benzene (AB) and hydrazo-benzene (HAB), as illustrated in Scheme 1. Hence, developing an efficient catalytic system for achieving high selectivity to *m*-NAN is a hot topic and has achieved some progress. For example, over 5% Pd/C, *m*-NAN was obtained with a 95% selectivity at 90% conversion at the conditions of 31 °C, 3.4 MPa H_2 [1]. Over 5% Pt/C, 97% selectivity to *m*-NAN was obtained at 48% conversion in supercritical CO_2 at 50 °C, 16 MPa [6]. Over Pd/C and Pt/C catalysts, the reaction condition has significant effects on the product selectivity. Supported Au catalysts, such as Au/Al_2O_3, Au/Fe_2O_3 and Au/TiO_2, could deliver 100% selectivity to *m*-NAN at about a 10% conversion of *m*-DNB [7–10]; however, the highest selectivity to *m*-NAN could not achieve 90% after conversion reached above 70%, due to *m*-NAN being further hydrogenated to *m*-PDA [5,8,11]. Ru/C was found to be efficient in the selective partial hydrogenation of *o*-, *m*- and *p*-DNBs, and the selectivities to the corresponding NANs achieved over 95% [3]. Ru/SnO_2 exhibits high selectivity (99.9%) in the hydrogenation of *o*-chloronitrobenzene, but the reaction rate was very low with a TOF of 4.3×10^{-2} s^{-1} [12]. The low activity was attributed to the high adsorption strength of the nitro group over Ru [13]. Recently, PVP-Ru/Al_2O_3 was discovered to be an effective catalyst for the partial hydrogenation of *m*-DNB to *m*-NAN with almost 100% selectivity at the conversion of *m*-DNB of <95%, and the addition of a metal cation, such as Fe^{3+} or Sn^{4+}, could markedly enhance the reaction rate and retain the high selectivity of *m*-NAN. The interaction between metal species may change the electronic density of the catalytic active site, thus affecting the adsorption state of the substrate on the catalyst surface [2].

Doping a second element to the supported transition metal catalysts is considered to be an efficient means, and a widely used one, to adjust the catalytic performance. Concerning the aforementioned supported Ru catalysts, modification with SnO_x, as an example, leads to wide applications in the hydrogenation of aliphatic acids [14,15], esters [16–22] and α,β-unsaturated carbonyl compounds [23–27]. It is suggested that SnO_x doping could improve the catalytic properties of Ru catalyst by the electronic and geometric effects of SnO_x [14,15]. Herein, we study the Ru-SnO_x/Al_2O_3 catalysts with varying SnO_2 loading in the range of 0%–3%. The effects of SnO_x on the structure and catalytic performance of Ru-SnO_x/Al_2O_3 catalysts are discussed in the hydrogenation of *m*-DNB. The catalysts are characterized by X-ray powder diffraction (XRD), X-ray photoelectron spectroscopy (XPS), transmission electron microscopy (TEM), hydrogen temperature-programmed reduction (H_2-TPR) and desorption (H_2-TPD).

Scheme 1. Possible reaction pathway for the hydrogenation of *m*-dinitrobenzene. *m*-DNB, *m*-dinitrobenzene; NNSB, *m*-nitro-nitrosobenzene; PHA, *m*-nitro-phenylhydroxylamine; *m*-NAN, *m*-nitroaniline; *m*-PDA, *m*-phenylenediamine; AOB, azoxybenzene; AB, azobenzene; HAB, hydrazobenzene.

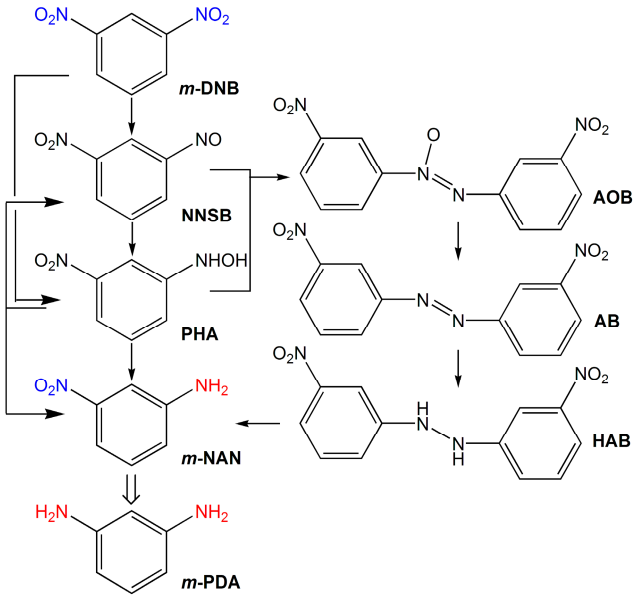

2. Results and Discussion

A series of supported Ru catalysts with different supports were prepared, and their catalytic performances on the hydrogenation of *m*-DNB were compared. The results are listed in Table 1. The Ru/TiO_2 catalyst presented the highest catalytic activity compared with other catalysts (Entry 1); it showed a 53% conversion in the reaction for 0.5 h with a TOF of 2142.7 h^{-1}. Compared with Ru/TiO_2, the activity of Ru/C was a little lower (TOF, 658 h^{-1}), and the other catalysts were quite low (TOF < 40 h^{-1}); they needed more than 5 h to achieve a similar conversion to that obtained with the Ru/TiO_2. However, for the catalytic selectivity to the desired product of *m*-NAN, the Ru/TiO_2 was less selective, while the Ru/Al_2O_3 was shown to be the most selective one, with selectivity above 97% (Entry 5). It is clear that the support has a significant influence on the catalytic activity and selectivity. Generally, a strong metal-support interaction exists in the supported noble metal catalysts, and it will affect the performance of the active species greatly, such as for the TiO_2-supported catalysts: the electron density around the metal particles decreased as the electron transferred (or polarized) from the metal nanoparticle to TiO_2 [28–30], and the electron-deficient state of the metal nanoparticle is favorable for the adsorption or hydrogenation of the nitro group [30–32]. Furthermore, the support has a great influence on the adsorption and desorption of the substrates, intermediates and products. When the formed intermediates of *m*-nitro-nitrosobenzene (NNSB) and PHA cannot be transferred to *m*-NAN in a timely manner, they may be desorbed from the catalyst, depending on the nature of the support, and condensed to AOB and then hydrogenated to AB and HAB, inducing a serious accumulation of these byproducts, due to their lower transferring rate to the final *m*-NAN.

Table 1. Results for the hydrogenation of *m*-DNB over supported Ru catalysts. Reaction conditions: *m*-DNB 2 mmol, catalyst 20 mg, EtOH 20 mL, H_2 4 MPa, 100 °C.

Entry	Catalyst	Time (h)	Conversion (%)	Selectivity (%)			Rate (h^{-1}) [b]
				m-NAN	*m*-PDA	Others [a]	
1 [c]	Ru/TiO_2	0.5	53.0	50.5	2.1	47.4	2142.7
2	Ru/C	1	86.0	74.8	2.9	22.3	434.6
3	Ru/SiO_2	5	35.6	56.9	0.5	42.6	36.0
4	Ru/kieselguhr	5	27.2	73.2	-	26.8	27.5
5	Ru/Al_2O_3	5	39.2	97.4	-	2.6	39.6

[a] Others are the by-products, such as PHA, AOB, AB, HAB; [b] Reaction rate unit: $mol_{m\text{-DNB}}/(mol_{Ru}\cdot h)$; [c] Catalyst 5 mg.

To improve the catalytic activity of Ru/Al_2O_3, the catalyst was modified with the addition of SnO_x, and the results are shown in Figure 1. It was found that the reaction activity increased obviously with the addition of SnO_x: with the increasing of the SnO_x loading from zero to 3%, the reaction rate was linearly increased; reaching the complete conversion of *m*-DNB was shortened gradually from 10 to 3 h. The selectivity to *m*-NAN was increased also: it reached 97.3% at a complete conversion for the catalyst with 2% SnO_x, but it decreased to 91.5% for the catalyst with 3% SnO_x, with the byproducts of AOB, AB and HAB being accumulated. Therefore, the optimal loading of SnO_x was 2%. The effects SnO_x on the structure of the $Ru\text{-}SnO_x/Al_2O_3$ catalysts and the catalytic performance were characterized and discussed by the results of XRD, TEM, H_2-TPR, H_2-TPD and XPS.

Figure 1. Selective hydrogenation of *m*-DNB to *m*-NAN over (**a**) Ru/Al_2O_3; (**b**) $Ru\text{-}SnO_x/Al_2O_3$-1%; (**c**) $Ru\text{-}SnO_x/Al_2O_3$-2%; and (**d**) $Ru\text{-}SnO_x/Al_2O_3$-3%. Reaction conditions: *m*-DNB 2 mmol, catalyst 20 mg, EtOH 20 mL, H_2 4 MPa, 100 °C. (■) conversion of *m*-DNB; selectivity to (○) *m*-NAN and (Δ) *m*-PDA; and (▽) others are by-products, such as PHA, AOB, AB and HAB.

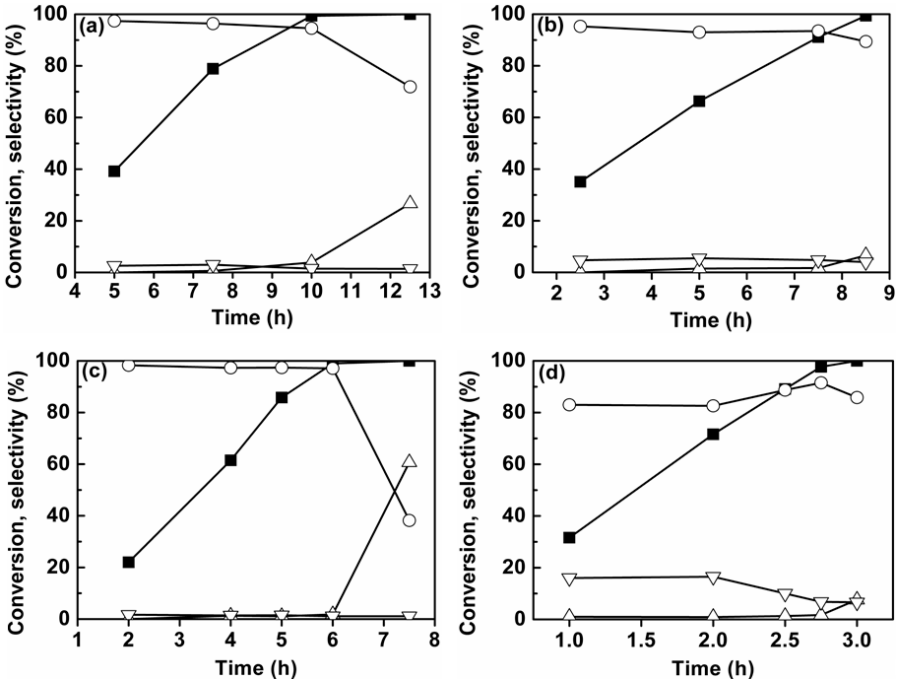

From the XRD patterns in Figure 2, the diffraction peaks appeared at 37.3°, 42.6°, 46.2° and 67.3° were attributed to γ-Al_2O_3 (Joint Committee on Powder Diffraction Standards (JCPDS), 13-0373), and the peaks at 38.4°, 42.2° and 44.0° were assigned to the metallic Ru^0 (JCPDS, 65-1863). With the addition and increase of the SnO_x loading, the diffraction strength of Ru was lowered, but the diffraction peaks of the Ru-Sn alloy, such as Ru_3Sn_7, Ru_2Sn_3 or $RnSn_2$, were not found, neither for the diffraction peaks of SnO_2 nor for those of SnO. Thus, we cannot determine the composition of SnO_x, and it may be an amorphous state existing in the samples.

Figure 2. XRD patterns of (**a**) Ru/Al_2O_3; (**b**) Ru-SnO_x/Al_2O_3-1%; (**c**) Ru-SnO_x/Al_2O_3-2%; and (**d**) Ru-SnO_x/Al_2O_3-3%. (●) γ-Al_2O_3; (▽) Ru^0.

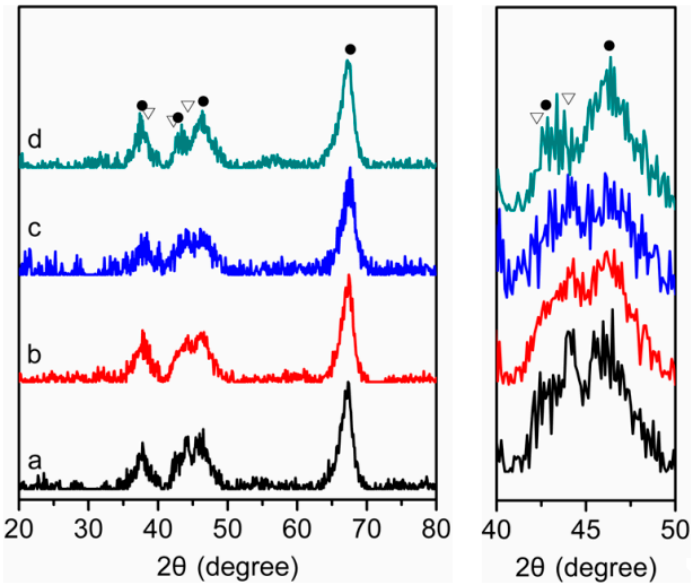

The TEM images and EDX spectra of supported Ru catalyst are shown in Figure 3. The average size of the Ru particles was about 5 nm for all of the catalysts checked, indicating that the addition of SnO_x did not affect the distribution of Ru. The HRTEM images of Ru-SnO_x/Al_2O_3-1% and Ru-SnO_x/Al_2O_3-2%, presented a clear and well-ordered single-crystal lattice, and the lattice spacing was about 2.05 Å, which is the same as Ru(101) (2.055 Å). Additionally, the formation of the Ru-Sn alloy was not detected; this is in agreement with the results of XRD in Figure 2. However, for Ru-SnO_x/Al_2O_3-3%, a single-crystal lattice of Ru(101) cannot be found. With the increase of the SnO_x loading, the crystallinity of Ru was lowered, and this is also in agreement with the results of XRD. The crystallinity of Ru and the loading of SnO_x may have a great influence on the adsorption and desorption of the substrates, intermediates and products, resulting in the higher catalytic activity and the highest selectivity to *m*-NAN (97.3%) at the complete conversion for the catalyst with 2% SnO_x. In addition, the EDX spectra of Ru-SnO_x/Al_2O_3-2% showed the emission of Ru and Sn, indicating that Sn was certainly doped onto the surface of the catalyst, even though SnO_x was not detected by the XRD (Figure 2).

Figure 3. TEM images of (**a**) Ru/Al_2O_3; (**b**) $Ru\text{-}SnO_x/Al_2O_3$-1%; (**c**) $Ru\text{-}SnO_x/Al_2O_3$-2%; (**d**) $Ru\text{-}SnO_x/Al_2O_3$-3%; and (**e**) the used $Ru\text{-}SnO_x/Al_2O_3$-2% and (**f**) EDX of $Ru\text{-}SnO_x/Al_2O_3$-2%.

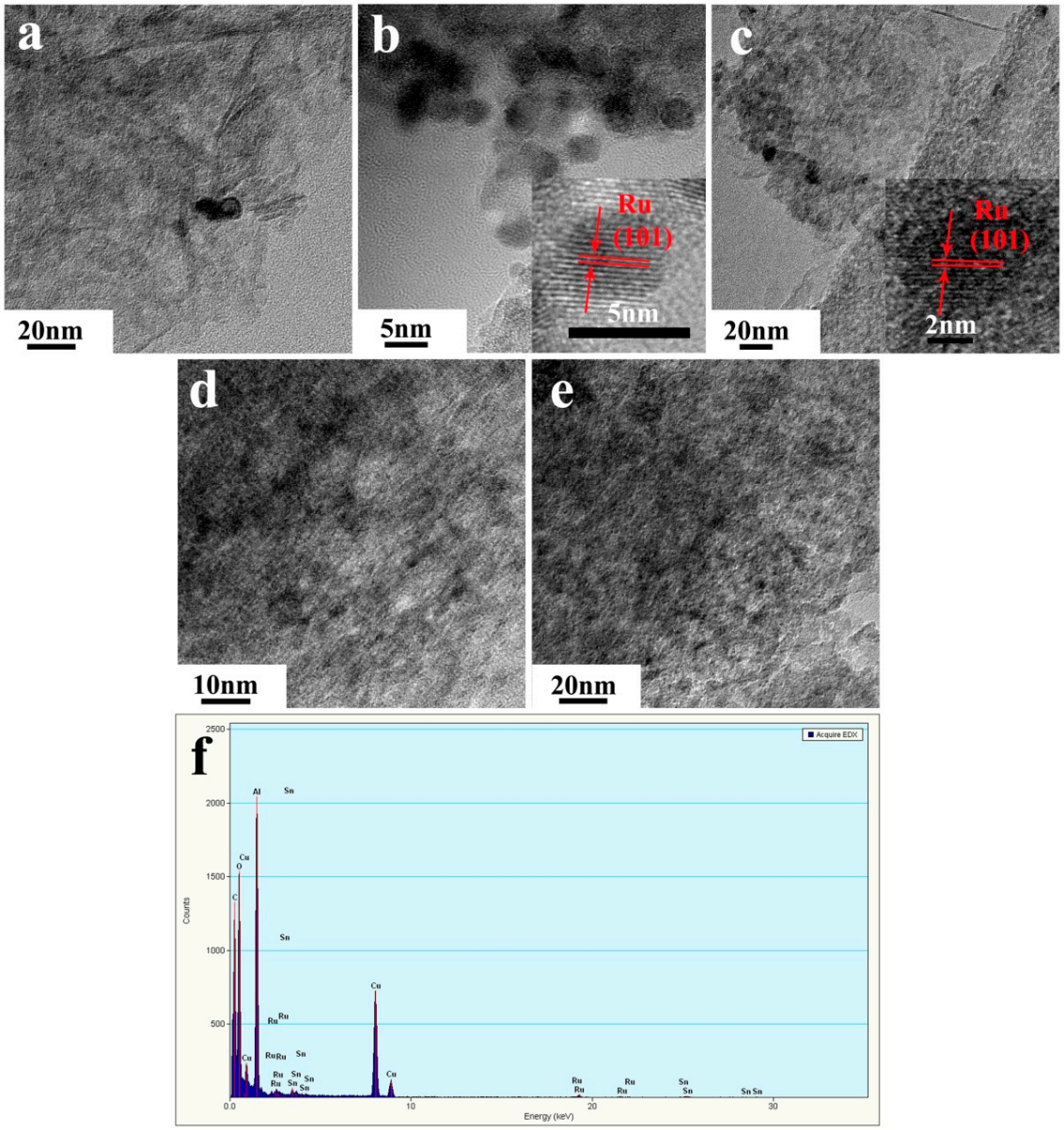

Figure 4 shows the H_2-TPR profiles of the supported Ru catalysts and SnO_x/Al_2O_3-2%. The SnO_x/Al_2O_3-2% presented a wide reduction peak at a temperature range of 100–650 °C. The reduction peaks at 198 °C are ascribed to SnO_x, which had a weak interaction with Al_2O_3, and the reduction peaks at 544 °C are ascribed to tin alumina, which was formed due to the strong interaction between SnO_x and Al_2O_3, which is favorable to the reduction of Sn^{4+} to Sn^{2+}, but inhibiting the further reduction of Sn^{2+} to Sn^0 [22,33]. For Ru/Al_2O_3, the reduction peaks at 85 °C are ascribed to Ru^{4+} to Ru^0, with the addition and increase of the SnO_x loading; the reduction peak and zone of Ru^{4+} changed slightly, and the reduction peaks at 198 °C ascribed to the overlapped SnO_x and the reduction peaks at 544 °C did not changed. This behavior also indicated that the Ru-Sn alloy was not formed. This is in agreement with the results of XRD and TEM. Figure 5 shows the H_2-TPD profiles of the supported Ru catalysts. With the increasing of the SnO_x loading, the area of the hydrogen desorption peaks increased,

indicating that the amount of the hydrogen adsorption increased due to the hydrogen spillover to the surface of SnO_x, resulting in an improvement of the hydrogenation activity.

Figure 4. The hydrogen temperature-programmed reduction (H_2-TPR) profiles of (**a**) SnO_x/Al_2O_3-2%; (**b**) Ru/Al_2O_3; (**c**) Ru-SnO_x/Al_2O_3-1%; (**d**) Ru-SnO_x/Al_2O_3-2%; and (**e**) Ru-SnO_x/Al_2O_3-3%.

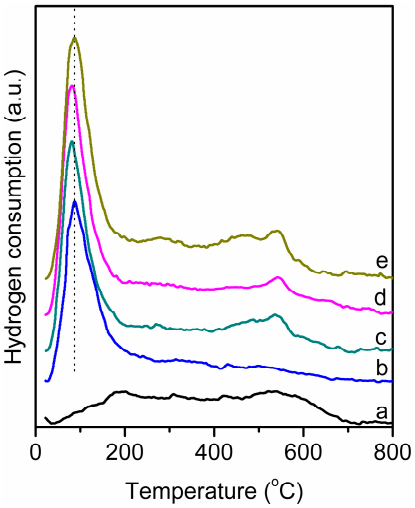

Figure 5. The H_2-TPD profiles of the supported Ru catalysts.

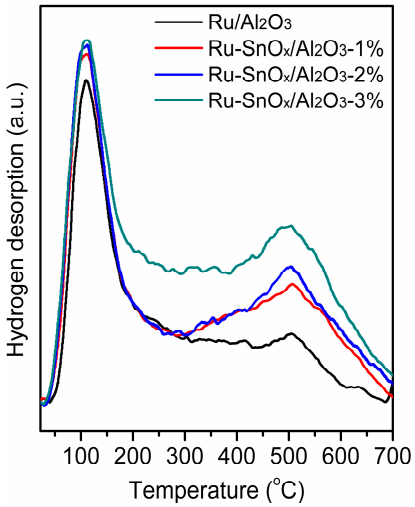

The XPS spectra of the supported catalysts are shown in Figure 6. In the case of Ru, because the Ru 3d spectra overlaps with the C 1s spectrum and the Ru $3p_{5/2}$ spectrum overlaps with the Sn $3d_{5/2}$ spectrum, the Ru $3p_{3/2}$ spectrum was used to deconvolute for all of the supported Ru catalysts. The metallic Ru at a binding energy of 462.6 eV was found for 2% Ru/Al_2O_3, as seen in Figure 6a [34]. With the addition and increase of the loading of SnO_x, the binding energy of Ru $3p_{3/2}$ moved to a higher binding energy, and this shifted to 463.2 eV for the sample with 3% SnO_x (Figure 6d). In the case of Sn, the binding energy of Sn $3d_{5/2}$ appeared at 487.2 eV in Ru-SnO_x/Al_2O_3-1%, which is ascribed to SnO; the metallic Sn and SnO_2 were not observed on the surface of the catalysts in this work, which is similar to the literature [34]. With the increasing of the loading of SnO_x, the binding energy shifted to a low value, and it moved to 486.9 eV for the sample

with 3% SnO_x. These results indicated that an electronic interaction existed between Ru and SnO_x: the electron transferred from Ru^0 to SnO_x, inducing the electron-deficient state of Ru nanoparticles for the Ru-SnO_x/Al_2O_3 catalysts. The electron-deficient state of the Ru nanoparticle is favorable for the adsorption of the electropositive nitrogen atom of the nitro group on the surface of the catalysts, and so, the N=O bond was activated [30–32]. The electron-deficient state of Ru may be also favorable for the adsorption of H_2 on its surfaces, resulting in the production of more active hydrogen species [32], thereby promoting the hydrogenation of *m*-DNB.

Figure 6. The XPS spectra of Ru $3p_{3/2}$ and Sn 3d of (**a**) Ru/Al_2O_3; (**b**) Ru-SnO_x/Al_2O_3-1%; (**c**) Ru-SnO_x/Al_2O_3-2%; and (**d**) Ru-SnO_x/Al_2O_3-3%.

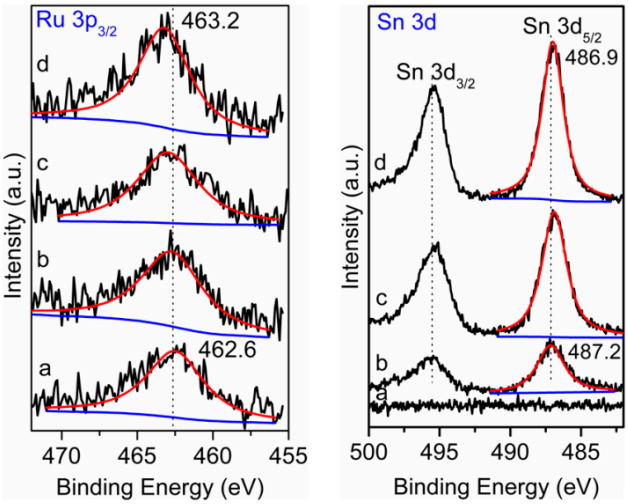

Figure 7. The recycling results of Ru-SnO_x/Al_2O_3-2% in the hydrogenation of *m*-DNB. Reaction conditions: *m*-DNB 2 mmol, catalyst 20 mg, EtOH 20 mL, H_2 4 MPa, 100 °C, 6 h.

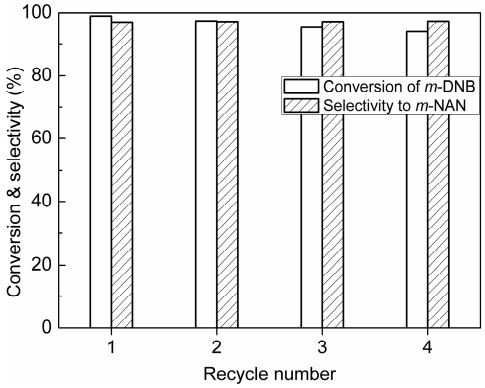

The stability of the Ru-SnO_x/Al_2O_3-2% catalyst was checked, as shown in Figure 7, the catalyst was shown to be relatively stable under the reaction conditions. The selectivity of *m*-NAN still remained above 97.3% in all of the recycling, although a slight decrease in the conversion appeared after the catalyst was reused four times, which may be ascribed to the loss of the catalyst during the catalyst separation in the recycling. For the heterogeneous catalysis, metal species leaching usually occurs during the reaction. In this work, Ru leaching was not detected in the filtrate based on the ICP-OES analysis with a detection limit of 0.1 ppm. Furthermore, TEM measurements showed that the Ru particles did not aggregate, and the average size of the Ru particles remained at about 5 nm for the

reused sample (Figure 3e). Therefore, the developed Ru-SnO_2/Al_2O_3-2% catalyst is an efficient catalyst for the hydrogenation of *m*-DNB with satisfactory activity, selectivity and stability; it is expected to have potential industrial applications.

3. Experimental Section

3.1. Materials

All chemicals were purchased from Aladdin (Shanghai, China); $SnCl_4 \cdot 5H_2O$, Na_2CO_3, ethanol and *m*-DNB were of analytical grade. γ-Al_2O_3 (170 m^2/g), TiO_2 (120 m^2/g), SiO_2 (Aldrich (Shanghai, China), 35-60 mesh, 150 Å), active carbon (Aldrich (Shanghai, China), 100–400 mesh) and kieselguhr were used as delivered. Gases of N_2 (99.999%), Ar (99.999%) and H_2 (99.999%) were purchased from Changchun Xinxing Gas Company (Changchun, China) and used as delivered.

3.2. Catalyst Preparation

In a typical preparation, γ-Al_2O_3 (1.9 g) and $SnCl_4 \cdot 5H_2O$ (0.4 mmol) were added to 20 mL H_2O and stirred at 70 °C, then excessive Na_2CO_3 (1.2 mmol) in 5 mL H_2O was dripped into the above solution, and continuously stirred for 2 h. The resulting precipitates were centrifuged and washed with deionized water and pure ethanol, respectively, and, finally, dried in vacuum at 80 °C for 6 h and calcinated in N_2 at 400 °C for 2 h. In this way, SnO_x/Al_2O_3-3% was prepared. Then, 3% SnO_x-Al_2O_3 (0.98 g) and $RuCl_3 \cdot 3H_2O$ (0.2 mmol) were added to 20 mL H_2O and stirred at 70 °C. Then, excessive Na_2CO_3 (0.9 mmol) in 5 mL H_2O was dripped into the above solution and stirred for 2 h. The resulting precipitates were centrifuged and washed with deionized water and pure ethanol, respectively, and, finally, dried in vacuum at 80 °C for 6 h, calcinated in N_2 at 400 °C for 2 h and reduced in H_2 at 300 °C for 2 h. Thus, the Ru-SnO_x/Al_2O_3-3% was prepared, in which the loading of Ru was about 2%, as determined by ICP analysis.

The Ru/Al_2O_3, Ru/SiO_2, Ru/TiO_2, Ru/C and Ru/kieselguhr were also prepared by the same process as described above, except for the addition of $SnCl_4 \cdot 5H_2O$.

3.3. Catalyst Characterization

The Ru and SnO_x loading in the catalysts was measured by inductively coupled plasma-optical emission spectroscopy (ICP-OES, iCAP6300, Thermo Waltham, MA, USA). The metallic state on the surface of the catalyst was examined by XPS (Thermo (Waltham, MA, USA) ESCALAB 250), and the surface composition of the samples was determined from the peak areas of the corresponding lines using origin fitting. Binding energies of the reference compounds and catalysts were measured using the C 1s peak (284.6 eV) of the adventitious carbon as an internal standard. XRD was performed with a D8 ADVANCE X-ray Diffractometer. TEM was performed using FEI Tecnai, G20 (Hillsboro, OR, USA). H_2-TPR and H_2-TPD were carried out on the TP-5080 (Tianjin Xianquan Industry and Trade Development Co., Ltd, Tianjin, China), with a thermal conductivity detector. Before the H_2-TPR run, 50 mg of the calcinated catalyst were loaded in the quartz tube and pretreated with nitrogen at 150 °C for 30 min. After cooling to room temperature, the sample cell was heated at a ramping rate of 10 °C/min to 800 °C in an atmosphere of a H_2/Ar mixture gas (30 mL/min). For the H_2-TPD test,

60 mg of the reduced catalyst were loaded in the quartz tube and pretreated with nitrogen at 150 °C for 30 min. After the catalyst cooled to room temperature, the absorption was conducted by flushing the sample in a H_2/Ar flow for 30 min. Then, the sample was swept with Ar for 1 h to remove physisorbed and/or weakly bound species. H_2-TPD was performed by heating the sample from room temperature to 700 °C in Ar with a ramp rate of 10 °C/min, and the TPD spectra were recorded. A liquid nitrogen trap was used to remove water formed during the tests.

3.4. Hydrogenation of m-Dinitrobenzene

Catalytic experiments of the selective hydrogenation of *m*-DNB were carried out in a 100-mL autoclave equipped with magnetic stirring. In a typical hydrogenation process, 2 mmol *m*-DNB, 20 mg Ru-SnO_x/Al_2O_3-2% catalyst and 20 mL ethanol were successively charged into the reactor. Then, the reactor was sealed and flushed three times with N_2 to remove the air. After flushing, the reactor was heated up to 100 °C. Hydrogen (4 MPa) was introduced, and then, the reaction mixture was stirred by an agitation speed of 1200 rpm for 2 h. It was certified that the diffusion limitation was removed completely under the present stirring. After the reaction, the liquid products were centrifuged and analyzed with a gas chromatograph (GC-Shimadzu-2010 (Kyoto, Japan), FID, Capillary column, Rtx-5 30 m × 0.25 mm × 0.25 μm) and identified by gas chromatography/mass spectrometry (GC/MS, Agilent (Santa Clara, CA, USA) 5890). The GC results were obtained using an internal standard method, and *o*-xylene was always used as the internal standard. For the recycling experiment, the reaction mixture of the first run was centrifuged and separated by decantation. Then, the solid catalyst was washed three times with solvent of ethanol, and the next run was started with the fresh *m*-DNB and ethanol. The boiling points of *m*-DAN (283 °C), *m*-DNB (301 °C) and *m*-NAN (306 °C) were high, and that of the condensing byproduct was much higher. Therefore, the temperature of the injector and detector used was 320 °C, and the temperature of the oven increased from to 290 °C (10 °C/min) and remained for 6 min at 290 °C. Under these conditions, all of the products can be detected.

4. Conclusions

The catalytic performance of the supported Ru catalysts was compared for the hydrogenation of *m*-DNB to *m*-NAN, and it was found that the support has a large effect on the reaction rate and product selectivity. Ru/Al_2O_3 exhibits a high selectivity of >97%, but its activity is much lower compared with the Ru/TiO_2. To improve the activity, selectivity and stability, the Ru/Al_2O_3 was modified by doping with SnO_x. As expected, the activity of the Ru-SnO_x/Al_2O_3 catalyst was improved significantly, and it could remain the high selectivity to *m*-NAN (>97%). It was confirmed that the adsorption amount of hydrogen increased with the increasing of the SnO_x loading from H-TPD, due to the hydrogen spillover. In addition, the electronic interaction between Ru^0 and SnO_x induced Ru^0 to be in an electron-deficient state, due to the transfer of an electron from Ru^0 to SnO_x, which is favorable for the adsorption of the nitro group and the attack of hydrogen, resulting in high hydrogenation activity. Moreover, the developed Ru-SnO_2/Al_2O_3-2% catalyst is also a stable catalyst for the hydrogenation of *m*-DNB to *m*-NAN without a loss in activity and selectivity after recycling four times. This presents great potential for industrial applications.

Acknowledgments

The authors gratefully acknowledge the financial support from NSFC 21273222 and 21202159 and from Jilin Provincial, China, 20100562.

Author Contributions

Haiyang Cheng and Fengyu Zhao contribute to the experiment design and the article writing and revising. Haiyang Cheng also contributes to all the experimental data collection, and Weiwei Lin, Chao Zhang and Xiaoru Li contribute to the product analysis, catalyst characterization and helpful discussion as well.

Conflicts of Interest

The authors declare no conflict of interest.

References

1. Khilnani, V.L.; Chandalia, S.B. Selective hydrogenation. II. *m*-dinitrobenzene to *m*-nitroaniliine using palladium on carbon as catalyst. *Org. Process Res. Dev.* **2001**, *5*, 263–266.
2. Zhao, S.L.; Liang, H.D.; Zhou, Y.F. Selective hydrogenation of *m*-dinitrobenzene to *m*-nitroaniline catalyzed by PVP-Ru/Al_2O_3. *Catal. Commun.* **2007**, *8*, 1305–1309.
3. Hou, J.; Ma, Y.H.; Li, Y.H.; Guo, F.; Lu, L.H. Selective partial hydrogenation of dinitrobenzenes to nitroanilines catalyzed by Ru/C. *Chem. Lett.* **2008**, *37*, 974–975.
4. Telkar, M.M.; Nadgeri, J.M.; Rode, C.V.; Chaudhari, R. Role of a co-metal in bimetallic Ni-Pt catalyst for hydrogenation of *m*-dinitrobenzene to *m*-phenylenediamine. *Appl. Catal. A* **2005**, *295*, 23–30.
5. Martínez, J.J.; Rojas, H.; Vargas, L.; Parra, C.; Brijaldo, M.H.; Passos, F.B. Hydrogenation of *m*-dinitrobenzene over Au catalysts on magnetic supports. *J. Mol. Catal. A* **2014**, *383*, 31–37.
6. Zhao, F.Y.; Fujita, S.; Sun, J.M.; Ikushima, Y.; Arai, M. Hydrogenation of nitro compounds with supported platinum catalyst in supercritical carbon dioxide. *Catal. Today* **2004**, *98*, 523–528.
7. Cardenas-Lizana, F.; Gomez-Quero, S.; Keane, M.A. Gas phase hydrogenation of *m*-dinitrobenzene over alumina supported Au and Au-Ni alloy. *Catal. Lett.* **2009**, *127*, 25–32.
8. Cardenas-Lizana, F.; Gomez-Quero, S.; Baddeley, C.J.; Keane, M.A. Tunable gas phase hydrogenation of *m*-dinitrobenzene over alumina supported Au and Au-Ni. *Appl. Catal. A* **2010**, *387*, 155–165.
9. Cardenas-Lizana, F.; Gomez-Quero, S.; Perret, N.; Keane, M.A. Gold catalysis at the gas-solid interface: Role of the support in determining activity and selectivity in the hydrogenation of *m*-dinitrobenzene. *Catal. Sci. Technol.* **2011**, *1*, 652–661.
10. Cardenas-Lizana, F.; Gomez-Quero, S.; Jacobs, G.; Ji, Y.; Davis, B.H.; Kiwi-Minsker, L.; Keane, M.A. Alumina supported Au-Ni: Surface synergism in the gas phase hydrogenation of nitro-compounds. *J. Phys. Chem. C* **2012**, *116*, 11166–11180.
11. Cardenas-Lizana, F.; Gomez-Quero, S.; Idriss, H.; Keane, M.A. Gold particle size effects in the gas-phase hydrogenation of *m*-dinitrobenzene over Au/TiO_2. *J. Catal.* **2009**, *268*, 223–234.

12. Zuo, B.J.; Wang, Y.; Wang, Q.L.; Zhang, J.L.; Wu, N.Z.; Peng, L.D.; Gui, L.L.; Wang, X.D.; Wang, R.M.; Yu, D.P. An efficient ruthenium catalyst for selective hydrogenation of ortho-chloronitrobenzene prepared via assembling ruthenium and tin oxide nanoparticles. *J. Catal.* **2004**, *222*, 493–498.
13. Wang, X.D.; Liang, M.H.; Zhang, J.L.; Wang, Y. Selective hydrogenation of aromatic chloronitro compounds. *Curr. Org. Chem.* **2007**, *11*, 299–314.
14. Zhu, Z.Q.; Lu, Z.H.; Li, B.; Guo, S.Z. Characterization of bimetallic Ru-Sn supported catalysts and hydrogenation of 1,4-cyclohexanedicarboxylic acid. *Appl. Catal. A* **2006**, *302*, 208–214.
15. Wettstein, S.G.; Bond, J.Q.; Alonso, D.M.; Pham, H.N.; Datye, A.K.; Dumesic, J.A. RuSn bimetallic catalysts for selective hydrogenation of levulinic acid to gamma-valerolactone. *Appl. Catal. B* **2012**, *117*, 321–329.
16. Ohnishi, T.; Yamakawa, T.; Shinoda, S. New preparation of Ru-Sn/Y zeolite catalyst for the formation of acetic acid (methyl acetate) from methanol alone. *Appl. Catal. A* **2002**, *231*, 27–33.
17. Dos Santos, S.M.; Silva, A.M.; Jordao, E.; Fraga, M.A. Performance of RuSn catalysts supported on different oxides in the selective hydrogenation of dimethyl adipate. *Catal. Today* **2005**, *107–108*, 250–257.
18. Corradini, S.A.D.; Lenzi, G.G.; Lenzi, M.K.; Soares, C.M.F.; Santos, O.A.A. Characterization and hydrogenation of methyl oleate over Ru/TiO_2, $Ru-Sn/TiO_2$ catalysts. *J. Non-Cryst. Solids* **2008**, *354*, 4865–4870.
19. Silva, A.M.; Morales, M.A.; Baggio-Saitovitch, E.M.; Jordao, E.; Fraga, M.A. Selective hydrogenation of dimethyl adipate on titania-supported RuSn catalysts. *Appl. Catal. A* **2009**, *353*, 101–106.
20. Miyake, T.; Makino, T.; Taniguchi, S.; Watanuki, H.; Niki, T.; Shimizu, S.; Kojima, Y.; Sano, M. Alcohol synthesis by hydrogenation of fatty acid methyl esters on supported Ru-Sn and Rh-Sn catalysts. *Appl. Catal. A* **2009**, *364*, 108–112.
21. Echeverri, D.A.; Marin, J.M.; Restrepo, G.M.; Rios, L.A. Characterization and carbonylic hydrogenation of methyl oleate over $Ru-Sn/Al_2O_3$: Effects of metal precursor and chlorine removal. *Appl. Catal. A* **2009**, *366*, 342–347.
22. Mazzieri, V.A.; Sad, M.R.; Vera, C.R.; Pieck, C.L.; Grau, R. Preparation and characterization of $Ru-Sn/Al_2O_3$ catalysts for the hydrogenation of fatty acid methyl esters. *Quim. Nova* **2010**, *33*, 269–272.
23. Hajek, J.; Kumar, N.; Salmi, T.; Murzin, D.Y.; Karhu, H.; Vayrynen, J.; Cerveny, L.; Paseka, I. Impact of catalyst reduction mode on selective hydrogenation of cinnamaldehyde over Ru-Sn sol-gel catalysts. *Ind. Eng. Chem. Res.* **2003**, *42*, 295–305.
24. Hajek, J.; Murzin, D.Y. Liquid-phase hydrogenation of cinnamaldehyde over a Ru-Sn sol-gel catalyst. 1. Evaluation of mass transfer via a combined experimental/theoretical approach. *Ind. Eng. Chem. Res.* **2004**, *43*, 2030–2038.
25. Hajek, J.; Maki-Arvela, P.; Toukoniitty, E.; Kumar, N.; Salmi, T.; Murzin, D.Y.; Cerveny, L.; Paseka, I.; Laine, E. The effect of chemical reducing agents in the synthesis of sol-gel Ru-Sn catalysts: Selective hydrogenation of cinnamaldehyde. *J. Sol-Gel Sci. Technol.* **2004**, *30*, 187–195.
26. Springerova, J.; Kacer, P.; Cerveny, L. Selective hydrogenation of alpha,beta-unsaturated carbonyl compounds on supported Ru-Sn catalysts. *Res. Chem. Intermed.* **2005**, *31*, 785–795.

27. Riguetto, B.A.; Rodrigues, C.E.C.; Morales, M.A.; Baggio-Saitovitch, E.; Gengembre, L.; Payen, E.; Marques, C.M.P.; Bueno, J.M.C. Ru-Sn catalysts for selective hydrogenation of crotonaldehyde: Effect of the Sn/(Ru + Sn) ratio. *Appl. Catal. A* **2007**, *318*, 70–78.
28. Li, D.; Ichikuni, N.; Shimazu, S.; Uematsu, T. Hydrogenation of CO_2 over sprayed Ru/TiO_2 fine particles and strong metal-support interaction. *Appl. Catal. A* **1999**, *180*, 227–235.
29. Li, X.H.; Zheng, W.L.; Pan, H.Y.; Yu, Y.; Chen, L.; Wu, P. Pt nanoparticles supported on highly dispersed TiO_2 coated on SBA-15 as an efficient and recyclable catalyst for liquid-phase hydrogenation. *J. Catal.* **2013**, *300*, 9–19.
30. Lin, W.W.; Cheng, H.Y.; Ming, J.; Yu, Y.C.; Zhao, F.Y. Deactivation of Ni/TiO_2 catalyst in the hydrogenation of nitrobenzene in water and improvement in its stability by coating a layer of hydrophobic carbon. *J. Catal.* **2012**, *291*, 149–154.
31. Zhang, J.L.; Wang, Y.; Ji, H.; Wei, Y.G.; Wu, N.Z.; Zuo, B.J.; Wang, Q.L. Magnetic nanocomposite catalysts with high activity and selectivity for selective hydrogenation of ortho-chloronitrobenzene. *J. Catal.* **2005**, *229*, 114–118.
32. Zhao, Y.F.; Zhang, H.Y.; Huang, C.L.; Chen, S.; Liu, Z.M. Pt/Titania/reduced graphite oxide nanocomposite: An efficient catalyst for nitrobenzene hydrogenation. *J. Colloid Interface Sci.* **2012**, *374*, 83–88.
33. Mazzieri, V.A.; Grau, J.M.; Yori, J.C.; Vera, C.R.; Pieck, C.L. Influence of additives on the Pt metal activity of naphtha reforming catalysts. *Appl. Catal. A* **2009**, *354*, 161–168.
34. Thepkaew, J.; Therdthianwong, S.; Therdthianwong, A.; Kucernak, A.; Wongyao, N. Promotional roles of Ru and Sn in mesoporous PtRu and PtRuSn catalysts toward ethanol electrooxidation. *Int. J. Hydrogen Energy* **2013**, *38*, 9454–9463.